

AD-A108 287

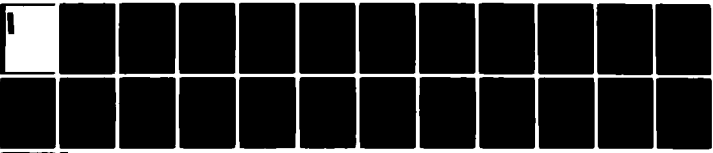
JAYCOR ALEXANDRIA VA F/G 20/7
SIMPLE ANALYSIS OF LIGHT ION BEAM LOSSES IN DEUTERIUM PLASMA CH--ETC(U)
NOV 81 D G COLOMBANT, S A GOLDSTEIN

UNCLASSIFIED

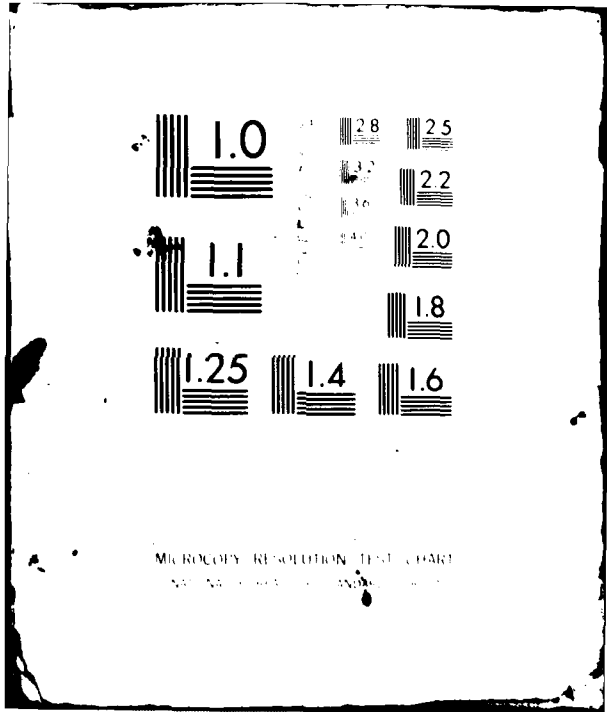
NRL-MR-4640

NL

1-1
4
A



END
DATE
FILMED
1 82
DTIC



MICROCOPY RESOLUTION TEST CHART
NBS 1963-A

AD A I 0 8 2 8 7

REPORT DOCUMENTATION PAGE		READ INSTRUCTIONS BEFORE COMPLETING FORM
1. REPORT NUMBER NRL Memorandum Report 4640	2. GOVT ACCESSION NO. AD-A108 257	3. RECIPIENT'S CATALOG NUMBER
4. TITLE (and Subtitle) SIMPLE ANALYSIS OF LIGHT ION BEAM LOSSES IN DEUTERIUM PLASMA CHANNELS	5. TYPE OF REPORT & PERIOD COVERED Interim report on a continuing NRL problem	
	6. PERFORMING ORG REPORT NUMBER	
7. AUTHOR(s) D. G. Colombant and S. A. Goldstein*	8. CONTRACT OR GRANT NUMBER(s)	
9. PERFORMING ORGANIZATION NAME AND ADDRESS Naval Research Laboratory Washington, DC 20375	10. PROGRAM ELEMENT, PROJECT, TASK AREA & WORK UNIT NUMBERS JO 47-0879-0-1 Sponsor Assignment No. DE-A 108-79DP40092	
11. CONTROLLING OFFICE NAME AND ADDRESS U.S. Department of Energy Washington, DC 20545	12. REPORT DATE November 16, 1981	
	13. NUMBER OF PAGES 29	
14. MONITORING AGENCY NAME & ADDRESS (if different from Controlling Office)	15. SECURITY CLASS. (of this report) Unclassified	
	15a. DECLASSIFICATION DOWNGRADING SCHEDULE	
16. DISTRIBUTION STATEMENT (of this Report) Approved for public release; distribution unlimited		
17. DISTRIBUTION STATEMENT (of the abstract entered in Block 20, if different from Report)		
18. SUPPLEMENTARY NOTES *Jaycor Inc., Alexandria, VA		
19. KEY WORDS (Continue on reverse side if necessary and identify by block number) Light ion beam propagation Beam transport efficiency Beam channel response		
20. ABSTRACT (Continue on reverse side if necessary and identify by block number) Simple analysis of both ion beam energy losses and beam current density reduction is presented for deuterium plasma channels. It is found that whereas an optimum density may exist for reducing the beam energy losses in the channel, no optimum density can be found to minimize the beam current density reduction. Plasma channel radius effects are then examined. It is found that the total ion beam energy loss is not strongly dependent on the initial channel radius. We conclude that final focusing elements in conjunction with channels initially at rest allow (Continued)		

DD FORM 1 JAN 73 1473

EDITION OF 1 NOV 65 IS OBSOLETE
S/N 0102-014-6601

SECURITY CLASSIFICATION OF THIS PAGE (When Data Entered)

612452

20. ABSTRACT (Continued)

for multiterawatt beams to be transported efficiently to 1 cm^2 targets while the channel cross-section can be larger.

CONTENTS

I.	Introduction.....	1
II.	Electric Field Generation	3
III.	B_z Field Modifications.....	6
IV.	Effects of Plasma Channel Radius.....	8
V.	Conclusion.....	10
	Acknowledgment.....	10
	References.....	11

Accession For	
No. 3-08581	<input checked="" type="checkbox"/>
DTIC TAB	<input type="checkbox"/>
Unannounced	<input type="checkbox"/>
Justification	
By	
Distribution/	
Availability Codes	
Avail and/or	
Spec	Special
A	

SIMPLE ANALYSIS OF LIGHT ION BEAM LOSSES IN DEUTERIUM PLASMA CHANNELS

I. Introduction

In a previous paper,¹ the magnetohydrodynamic response of plasma channels to propagating light ion beams has been investigated. The half a centimeter radius channels were assumed to be deuterium at around 10^{-5} g/cm with 50 nsec pulses of .4-1MA/cm², 3-5 MeV proton beams injected into them. Basic phenomena like beam collisional energy losses, heating of the channel, expansion of the channel due to beam pressure and the resulting reduction in confinement were shown to take place over the duration of the beam pulse. While a window on the plasma density was given, no optimum for propagation was defined. In this paper, we present a simple analysis to optimize power density transport of the ion beam through the channel and show when such an optimization process is possible. In particular, we concentrate on the energy delivery at the tail of the beam because both voltage and current are highest at that time (as a result of bunching requirements.) We consider separately the ion beam total energy losses and the current density reductions in the plasma channel. We look successively into these two areas and combining them together, we look into the optimization of the power density after transport in the channel.

This analysis applies primarily to deuterium plasma channels where radiation losses are assumed to be negligible. If the beam pulse length were short enough or the plasma channel density high enough, negligible motion would be induced into the channel by the beam over the pulse duration of the beam pulse. However for very short beam pulse length, not enough energy would be available in the beam. For high channel density, beam energy losses would be too large and therefore one must decrease the channel density and allow channel motion on the time scale of the beam pulse duration. This motion then changes the channel confinement characteristics.

Two kinds of effects are thus to be considered: energy losses and beam current density reductions. The beam energy losses are due to decelerating electric fields in addition to the binary collisional energy losses and beam current density reductions are related to the plasma channel radial expansion. These two different kinds of effects will be treated separately. Combined together, they lead to a new concept of overall transport efficiency which we define as

$$\eta_{tr} = \eta_e \eta_J = \frac{\epsilon_{out}}{\epsilon_{in}} \frac{J_{out}}{J_{in}} \quad (1)$$

where J refers to beam current density, ϵ to beam energy (MeV/proton), "out" to values at the end of the channel and "in" at the channel entrance (beam injection values).

A brief examination of the channel parameters shows that the plasma density in the channel and the plasma channel radius just prior to beam injection are some of the easiest to change. Parameters which characterize channels are chemical composition, magnitude of the current I_{ch} which flows through them, current density profile $j_{ch}(r)$, radius r_{ch} , mass density distribution $\rho(r)$ and also radial velocity distribution in the channel $v(r)$ prior to beam injection. Recently, imploding channels² have also been proposed as a medium for transporting ion beams and they are presently under investigation. In the present paper, we confine ourselves to the following choices: Deuterium gas constitutes the background channel material in order to be able to neglect radiation losses. The channel discharge current follows from the beam characteristics only and is given by $I_{ch}(A) \approx .5 \cdot 10^{-3} \theta_m^2 V_0$ (cm/sec) where θ_m is the maximum beam injection angle and V_0 the ion beam initial velocity. The current density is assumed to be uniform up to the channel radius. In a light ion beam transport scheme,^{3,4} the beam is first focused then transported at a radius comparable to the target radius before hitting the target. Different possibilities for the relationship between the channel and the target radii are described later in this paper. The channel configuration has been assumed to be a z-discharge initially at rest ($v_r = 0$ at $t = 0$). This has been shown to be experimentally and theoretically MHD stable on the channel formation time of a few μ sec.^{5,6} The mass density radial distribution in the channel prior to beam injection is assumed to be independent of the radius. Its magnitude can be varied over several orders of magnitude up to a limit ρ_a when energy losses become too large. This value is given by

$$\rho_a SL = \alpha \epsilon \quad (2)$$

where S is the binary collisional stopping power, L is the length over which the beam is to be transported, and α is the fraction of the initial beam energy which is allowed to be lost during transport. For fully ionized deuterium, $S \approx 10^3/\epsilon$ MeV/g/cm² where ϵ is the proton energy in MeV. The transport length L derived from bunching considerations is

$$L \left(\frac{1}{v_0} - \frac{1}{v_r} \right) = \tau \quad (3)$$

where v_0 and v_r are respectively the ion velocities at the head and the tail of the beam and τ is the beam pulse duration, all these quantities being defined at the channel entrance. For $v_r = 2v_0$ (energy ramp increasing to twice its initial value), $L(\text{cm}) = 3.3 \cdot 10^9 \epsilon \tau$ (sec). Combining Eqs. (2) and (3), we find a value for ρ_a equal to

$$\rho_a = \frac{\alpha \cdot 3 \cdot 10^{-13} \epsilon^{3/2}}{\tau} \quad (4)$$

For $\epsilon = 5$ MeV, $\tau = 50$ nsec, and $\alpha = 20\%$, $\rho_a = 1.3 \cdot 10^{-5}$ g/cm³.

A minimum density must also be achieved in the channel in order to ensure charge and current neutralization and also not to excite electrostatic instabilities. If such instabilities are excited, the plasma resistivity becomes much larger than Spitzer resistivity which causes an increase in the net current as well as large electric fields. If these instabilities are not excited, Spitzer resistivity can be assumed and typical diffusion time of the net current are of the order of a few μ sec. Thus during a typical beam pulse, a net current of the order of 1% of the beam current will be added to the channel as was observed in numerical solutions.¹ To avoid electrostatic instabilities,⁷ $n_p \geq 5 \times 10^{17}$ for the above parameters. This minimum density is about an order of magnitude smaller than ρ_a given in the example above, hence no plasma instabilities occur if more than a few % fractional energy loss is allowed.

II. Electric Field Generation

At $t < 0$, there is a small electric field in the channel corresponding to I_{ch} . As the beam enters the channel, electric fields from various sources develop. From the generalized Ohm's law, they are

due to channel expansion with velocity v_p which leads to $v_p B/c$ and plasma resistivity. In addition, there is an equivalent electric field due to beam energy collisional deposition.

The electric field terms are all negative with the possible exception of the first one for an imploding channel. The energy losses can be written

$$\frac{dE}{dx} = \left[\frac{v_p B}{c} \right] + \rho S + \eta j_p$$

where the brackets mean average over an ion betatron orbit. The first term goes from 0 at the channel center ($B = 0$, $v = 0$) to a maximum value at the channel boundary where v_p and B usually reach their maximum. For the purpose of the present simple analysis, a mean value is used for this term which is equal to 1/2 of its maximum value. Term by term, the electric field is thus:

$$a) \frac{\langle v_p B \rangle}{c}$$

From Ref. 1, we get $v_p \approx \frac{t j_b B}{\rho_0 c}$. However, this relation is correct to zeroth order only. If we take into account the fact that the mass density decreases due to expansion, then to first order, the expression for the radial velocity becomes

$$v_p \approx \frac{t j_b B_0}{c \rho_0 (1 + \chi)} \quad (5)$$

where

$$\chi = \frac{3 \cdot 10^{-2} j_b \alpha j_{ch0} t^2}{\rho_0} \quad (6)$$

is the expansion parameter and the 0 subscripts refer to channel and beam conditions at injection. The reduced velocity is due to the fact that the $(j \times B)$ term driving the expansion decreases with radius faster than the mass density (the current density decreases in the same way as the mass density and the B field decreases by a factor $(1 + \chi)$ as will be shown in Sec. III). Now $B_0 = \frac{l_{ch}}{5r_0}$, so that

$$\frac{\langle v_p B \rangle}{c} = \frac{v_p B}{2c} \approx 6.4 \cdot 10^{-11} \frac{j_b \alpha j_{ch0} l_{ch0} t}{\rho_0 (1 + \chi)^2} \quad (7)$$

Note that this term is inversely proportional to ρ_0 for small χ and proportional to ρ_0 for large χ . Our simple analysis does not apply to that latter case.

b) ρS .

This term is simply $\frac{\rho_0}{(1+\chi)^2} \frac{10^9}{\epsilon}$ V/cm for protons in deuterium with $T_e \geq 1$ eV. It is proportional to ρ_0 for small χ and becomes proportional to ρ_0^3 for large values of χ (which correspond to small ρ_0).

c) ηj_p .

Using Spitzer resistivity justified by operating at densities around 10^{18} cm $^{-3}$ to avoid instabilities, this term is proportional to $\frac{Z \ln \Lambda}{T_e^{3/2}} j_p$ where the plasma return current density j_p has been assumed to be equal in magnitude to the beam current density j_b . Due to the small net current ($j_{cn} \ll j_b$) the most critical quantity to determine in this expression is T_e . Assuming no radiation losses, we know from Ref. 1 that $T_e \approx 3.5 \cdot 10^3 \frac{j_{b0} t}{\epsilon}$ so that for $\chi \ll 1$,

$$\eta j_b \approx 7.7 \cdot 10^{-8} \frac{\epsilon^{3/2}}{j_{b0}^{1/2} t^{3/2} (1+\chi)} \text{ V/cm} \quad (8)$$

where t is in sec and j_{b0} in A/cm 2 . An order of magnitude estimate shows that this resistive electric field is equal to 40 V/cm for $j_{b0} = 10^6$ A/cm 2 , $t = 50$ nsec and $\epsilon = 3$ MeV. Its dependence on density is very weak for small χ . Collecting all the terms, the total energy losses may then be written as

$$\frac{dE}{dx} = \frac{A}{\rho_0 [1+\chi(t)]^2} + \frac{B \rho_0}{[1+\chi(t)]^2} + \frac{C \epsilon^{3/2}}{j_{b0}^{1/2} t^{3/2} [1+\chi(t)]} \quad (9)$$

From the first two terms, we see that $\frac{dE}{dx}$ may reach a minimum as a function of ρ_0 for small χ . We find that this minimum is reached for

$$\rho_0 = \left(\frac{1-\chi}{1+3\chi} \right)^2 \left(\frac{A}{B} \right)^{1/2} \quad (10)$$

Note that $\chi \leq 1$ is a necessary condition for a minimum to exist. For small χ , the density corresponding to this minimum is

$$\rho_0 = \left(\frac{A}{B} \right)^{1/2} = \frac{1.4 \cdot 10^{10} t^{1/2} j_{b0}^{1/2} I_{c0} \epsilon^{1/2}}{r_{c0}} \quad (11)$$

This expression physically equates the energy losses due to binary collisions to the energy losses associated with the plasma expansion. Going back to the general case, since we have seen that χ is a function of ρ_0 , Eq. (10) is an implicit equation for ρ_0 . Eliminating this ρ_0 between Eqs. (7) and (10), a relationship between the various beam parameters when a minimum in the electric field occurs is obtained

$$j_{b_0} t^3 = 2.2 \cdot 10^{-14} r_{ch_0}^2 \epsilon \chi^2 \left(\frac{1 - \chi}{1 + 3\chi} \right). \quad (12)$$

This equation shows that when a minimum E field exists, a given fractional expansion χ sets a relationship between the beam pulse duration and the beam current density. A complete solution to Eq. (9) is shown in Figs. 1 and 2. It corresponds to $j_{b_0} = 1 \text{ MA/cm}^2$, $I_{ch_0} = 50 \text{ kA}$, $r_{ch_0} = 0.56 \text{ cm}$, $\epsilon_b = 3 \text{ MeV}$ in Fig. 1 and $\epsilon_b = 5 \text{ MeV}$ in Fig. 2. We find indeed that the minimum in the electric field exists only for small pulse durations. From Eq. (12) it is apparent that $j_{b_0} t^3$ has a maximum as a function of χ which occurs for $\chi = .6$. For longer pulse durations or larger j_{b_0} there will be no minimum in the electric field. This happens for $t \geq 25 \text{ ns}$ in the example of Fig. 1. At the same time that the minimum disappears, the expansion increases and while the beam current density decreases the electric field losses decrease also. For bunched cases, ($j_{b_0} t = \text{const}$), we see from Eq. (12) that a minimum will be reached more easily since now t^2 is smaller. It is important to keep the resistive term in the electric field at shorter pulse durations (unbunched) since in that case, the resistivity can be significant because the beam did not have time to heat up the channel to large temperatures. The expression for the energy efficiency follows directly from Eq. (9). It can be written as

$$\eta_\epsilon = \frac{\epsilon_{\text{out}}}{\epsilon_{\text{in}}} = \frac{\epsilon_{\text{in}} - EL}{\epsilon_{\text{in}}} = 1 - \frac{EL}{\epsilon_{\text{in}}}.$$

Using typical E -field values of Fig. 1, $E = 1.5 \text{ kV/cm}$, $L = 3 \text{ m}$ and $\epsilon_b = 3 \text{ MeV}$, η_ϵ equals 85%.

III. B_z Field Modifications

At $t < 0$, the B_z -field configuration is assumed to be that shown in Fig. 3a. It corresponds to a uniform channel current density following the formation of a low temperature channel where the magnetic field had time to diffuse. After beam injection, we assume that the temperature of the channel

has increased due to beam deposition and that the expansion is self-similar (the velocity increases linearly from the center to the edge of the channel). Because of the large conductivity due to channel heating, we assume that the B -field has been convected out with the plasma channel and that the maximum B -field is now reached at $r(1+\chi)$ as shown in Fig. 3b. Its maximum value has decreased from B_0 to $B_0/(1+\chi)$ since the same total current I_{ch} is assumed to flow in the channel. In fact, this assumption keeps the total flux $\int Bdr$ constant and the beam stays confined. We assume that the beam adjusts instantly to new channel conditions and that the change in beam radius follows the change in channel radius. Thus, because of the expansion, the current density is reduced by a factor $(1 + \chi)^2$. This model assumes a free channel expansion and does not take into account the fact that there can be a sharp density jump at the channel boundary, nor that the temperature has remained low in the outer region leading to diffusion of the B -field there.

The current density reduction factor is thus

$$\eta_J = \frac{J_{out}}{J_{in}} = \frac{1}{(1 + \chi)^2}. \quad (13)$$

In the present form (no ∇p effects on χ), it does not depend on beam energy. It does not show any extremum and leads to low values of η_J ($\leq 50\%$) when channel expansion occurs ($\chi \geq 0.4$). This current density drop due to channel expansion may be more restrictive than electric field losses as seen in Fig. 4.

We can now combine the energy transport efficiency η_e and η_J in one quantity defined as:

$$\eta_{tr} = \eta_e \eta_J.$$

This expression can be written in terms of first order quantities again and the analysis is quite lengthy. It can be shown that a maximum for η_{tr} occurs as a function of ρ_0 . Physically, it happens because η_e decreases for increasing ρ_0 while η_J increases. An implicit equation for this optimum value of the density is given by

$$\rho_0 = \frac{(1-C')(1+\chi)^2\chi \pm \sqrt{(1-C')^2(1+\chi)^4\chi^2 + A'B'(1+5\chi)(1+3\chi)}}{A'(1+5\chi)}$$

where

$$A' = AL/\epsilon$$

$$B' = BL/\epsilon$$

$$C' = C\epsilon^{1/2}L/(j_{b0}t)^{1/2}.$$

Figures 5 and 6 show η_{tr} for the same parameters as used in Figs. 1 and 2. We see that the maximum occurs for increasing ρ_0 as the beam pulse duration increases and that this maximum is very broad. The maximum values for η_{tr} depend on the energy of the beam which affects the energy transport efficiency. These calculations have been made for a 3 m long channel — longer channels would reduce the energy efficiency further. For these conditions, we see that it is difficult to achieve an overall η_{tr} greater than 50% for long pulses ($t \geq 40$ nsec). In order to increase the total efficiency, it is necessary to consider transport schemes that have the following options:

- a) the channel expansion is limited by means such as surrounding gas blanket or magnetic field.
- b) the channel implodes initially.
- c) the channel is allowed to expand but is followed by a focusing element.⁸

IV. Effects of Plasma Channel Radius

The previous analysis has been made supposing that the plasma channel radius was 0.56 cm initially (corresponding to an area of 1 cm²). However, the conclusions just reached suggest the use of a focusing element after the transport plasma channel as one possibility. This solution has very important implications for the whole transport scheme concept. It indicates that a) constraints on the channel radius can be relaxed and transport can be performed at a radius larger than the target radius b) current density reductions can be compensated for by focusing the beam at the end of the channel whereas energy losses cannot. In this section, we look briefly at the influence of channel radius on both energy losses and transport total efficiency. The formulation is the same as that used previously. We just

replace the beam and channel current densities by the beam and channel total current divided by πr_{ch0}^2 .

The total efficiency can then be written

$$\eta_{tr} = \frac{1}{\left[1 + \frac{\alpha}{r_{ch0}^4}\right]^2} \left[\frac{\left[\frac{A''}{\rho_0 r_{ch0}^4 \left[1 + \frac{\alpha}{r_{ch0}^4}\right]^2} + \frac{B\rho_0}{\left[1 + \frac{\alpha}{r_{ch0}^4}\right]^2} + \frac{C'' r_{ch0}}{\left[1 + \frac{\alpha}{r_{ch0}^4}\right]} \right] L}{\epsilon_{in}} \right] \quad (14)$$

where

$$\alpha = 3.10^{-3} I_{b0} I_{ch0}^2 / \rho_0$$

$$A'' = 6.4 \times 10^{-12} I_{b0} I_{ch0}^2 t$$

$$C'' = 1.77 C \epsilon_{in}^{3/2} / (I_{b0}^{1/2} t^{3/2}).$$

Note the 4th power dependence on r_{ch0} which comes into various terms and which has been pointed out in the expansion parameter χ previously. In general, it is complicated to see the effects of channel radius on either the energy losses or the transport total efficiency. Solutions to Eq. (14) appear in Fig. 7 for the energy loss efficiency and in Fig. 8 for the transport total efficiency as a function of r_{ch0} and ρ_0 for the following parameters: $I_b = 1$ MA, $I_{ch} = 50$ kA, $\epsilon_i = 3$ MeV, $t = 40$ nsec, $L = 3$ m. The effects of the plasma channel radius are now more easily apparent. The energy loss efficiency depends weakly on the channel radius at low channel density as shown in Fig. 7. In general, using small radii causes the plasma to expand so that the final radius does not depend strongly on initial radius. The curves drop as a functions of ρ_0 because of the collisional energy losses.

As for the overall transport efficiency, note in Fig. 8 the S-shape of the curves. At small radii, current densities increase and channel expansion can be large leading to small η_J . At large radii, current densities decrease as well as channel expansion and η_{tr} becomes equal to η_e . Increasing the channel radius to more than 1.2 cm at $\rho_0 = 10^{-6}$ g/cc or to more than 0.6 cm at $\rho_0 = 1.6 \cdot 10^{-5}$ g/cc will not bring any significant increase in the value of η_{tr} . At these radii, the decrease in η_{tr} with ρ_0 is due to the decrease in η_e with ρ_0 .

Notice that these results are given at $t = 40$ nsec while previous results were given as a function of time.

V. Conclusion

We have shown that in order to minimize electric field losses in a plasma channel where a high intensity light ion beam is injected an optimum density exists for low- Z material and short pulses. We have also shown that no optimum density minimizes reduction in current density associated with the outward convection of the B -field. Finally, we have seen that an optimum density may exist for the overall beam energy flux efficiency.

A practical way of choosing the initial channel density in a channel initially at rest is to ensure that it remains close to ρ_0 which is the maximum allowable beam energy degradation, thus providing the highest inertia to beam-induced motion and limiting changes in the initial B -field.

In order to increase the overall beam power density transport efficiency one of the following schemes needs to be considered: channel surrounded by gas blanket, imploding channels and finally channel followed by focusing element. The advantage of this latter scheme is that it can cancel completely in principle the reduction in current density, leaving only energy losses in the channel which depend only weakly on channel radius. For example, the case of $I_b = 1$ MA, $I_{ch} = 50$ kA, $L = 3$ m, $r = 0.56$ cm shows an overall efficiency less than 50% for beam pulses longer than 40 nsec. However, when this same beam current is allowed to propagate in a channel of 1 cm radius for example followed by a focusing element, then the overall efficiency can get as high as 90%.

Acknowledgment

This work was supported by the Department of Energy.

References

1. D.G. Colombant, S.A. Goldstein, and D. Mosher, *Phys. Rev. Lett.* **45**, 1253 (1980).
2. S.A. Goldstein and D.A. Tidman, *Proc. IEEE Int. Conf. on Plasma Science, Madison, Wisc.* (1980).
3. S.A. Goldstein, D.P. Bacon, D. Mosher, and G. Cooperstein, *Proc. Second Int. Conf. on High Power Electron and Ion Beam Res. and Tech., Ithaca, N.Y.* (1977).
4. P.A. Miller, L. Baker, J.R. Freeman, L.P. Mix, J.W. Poukey, and T.P. Wright, *ibid.*
5. F.L. Sandel, F.C. Young, S.J. Stephanakis, W.F. Oliphant, G. Cooperstein, S.A. Goldstein, and D. Mosher, *Bull. Am. Phys. Soc.* **25**, 900 (1980); J.N. Olsen, D.J. Johnson, and R.J. Leeper, *Appl. Phys. Lett.* **36**, 808 (1980).
6. W.M. Manheimer, M. Lampe, and J.P. Boris, *Phys. Fluids* **16**, 1126 (1973).
7. P.F. Ottinger, S.A. Goldstein and D. Mosher, *NRL Memorandum Report 4548* (1981).
8. P.F. Ottinger, S.A. Goldstein, and D. Mosher, *Proc. IEEE Int. Conf. on Plasma Science, Madison, Wisc.* (1980).

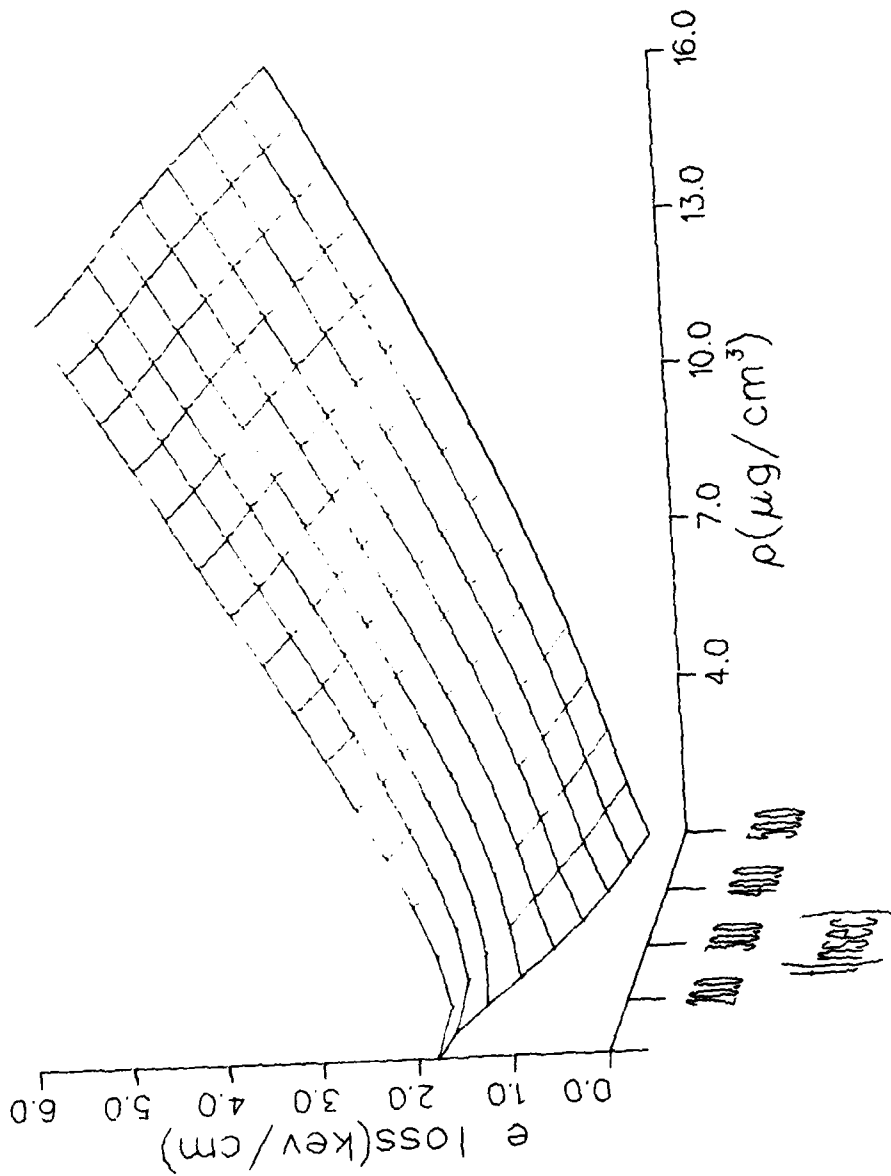


Fig. 1 - Energy losses in keV/cm as a function of beam pulse duration and background channel density for the following parameters $J_{b0} = 1 \text{ MA/cm}^2$, $f_{ch0} = 50 \text{ kA}$, $r_{ch0} = 0.56 \text{ cm}$, and $\epsilon_b = 3 \text{ MeV}$

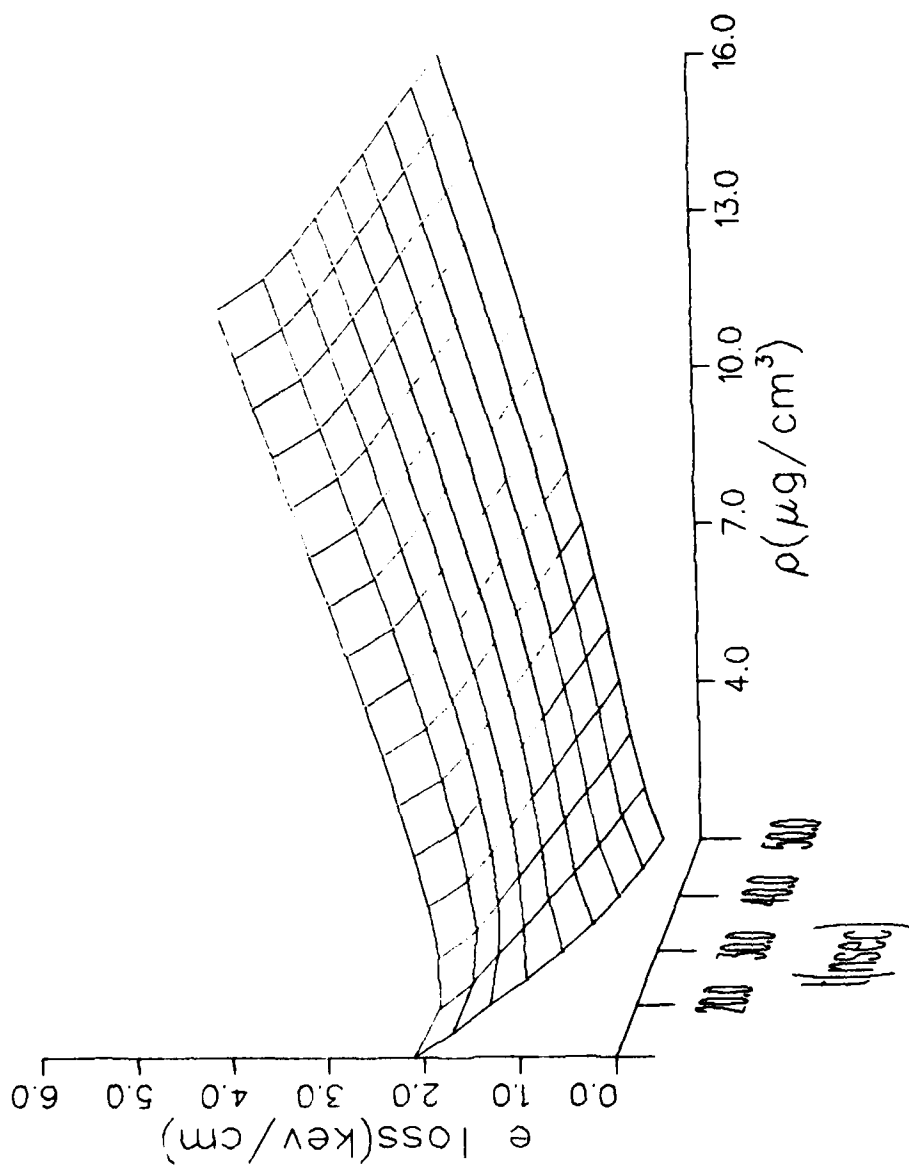


Fig. 2 — Same as in Fig. 1 for $\epsilon_0 = 5 \text{ MeV}$

a) $t = 0$

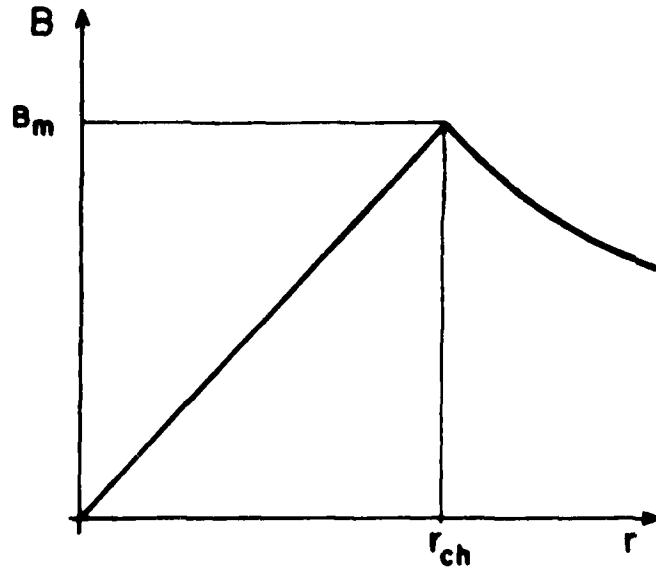
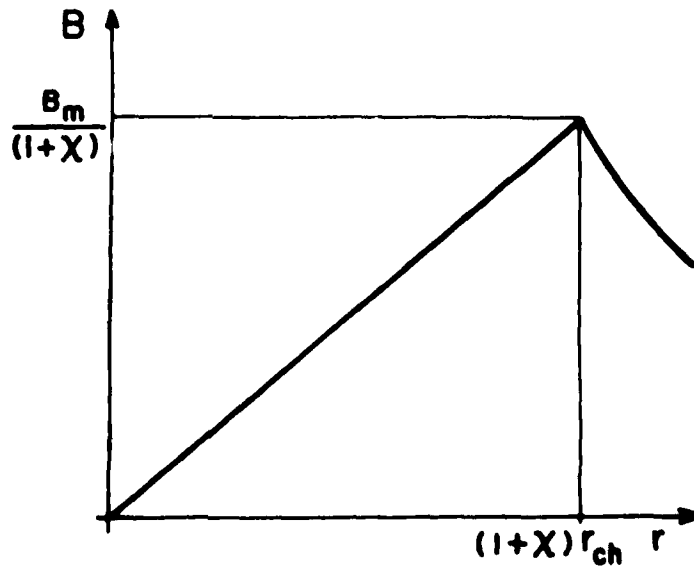


Fig. 3 - (a) Magnetic field configuration in the channel before beam injection (corresponding to uniform channel current density)

b) $t = \tau$



(b) Magnetic field configuration in the channel after beam injection (corresponding to same net current and taking into account channel expansion)

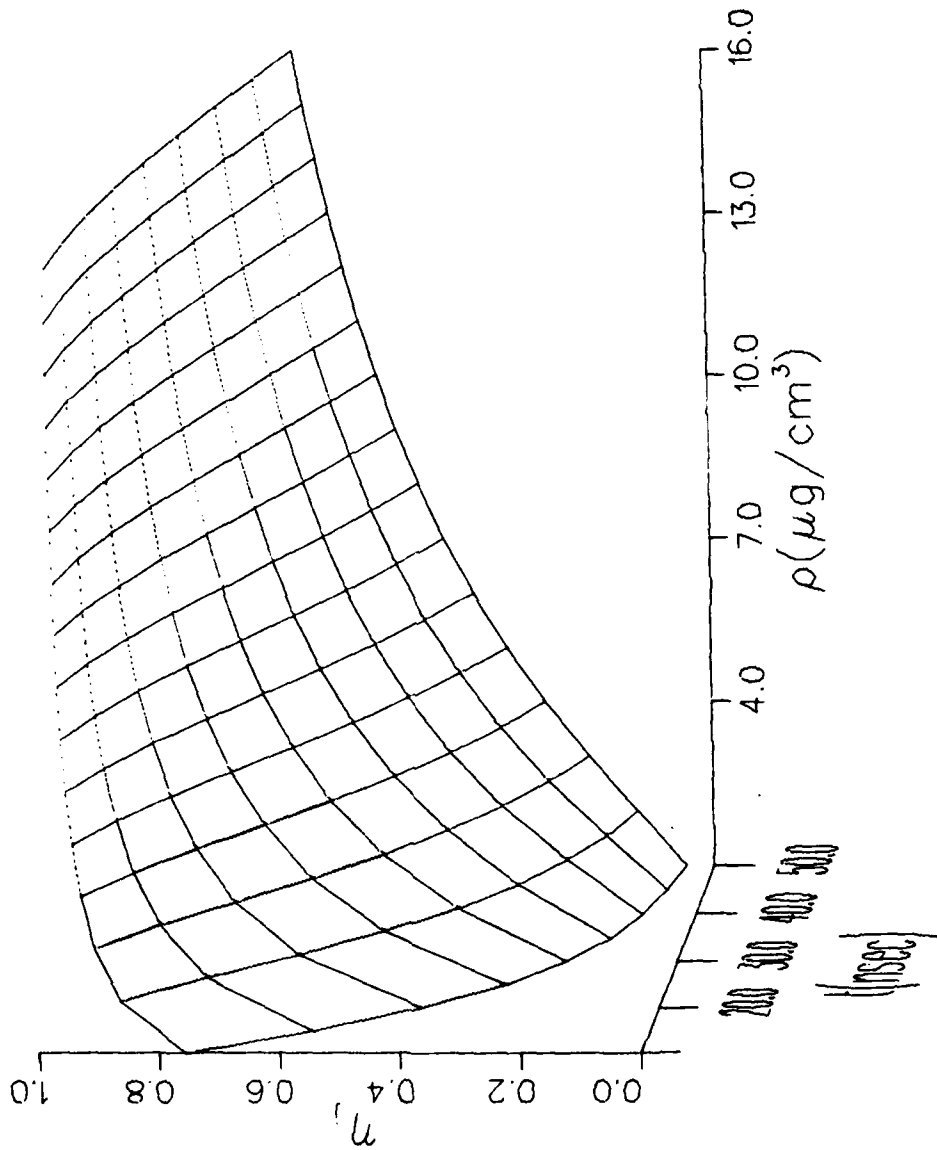


Fig. 4 - Current density reductions as a function of beam pulse duration and background channel density for the same parameters as in Fig. 1 (this curve does not depend on ion beam energy)

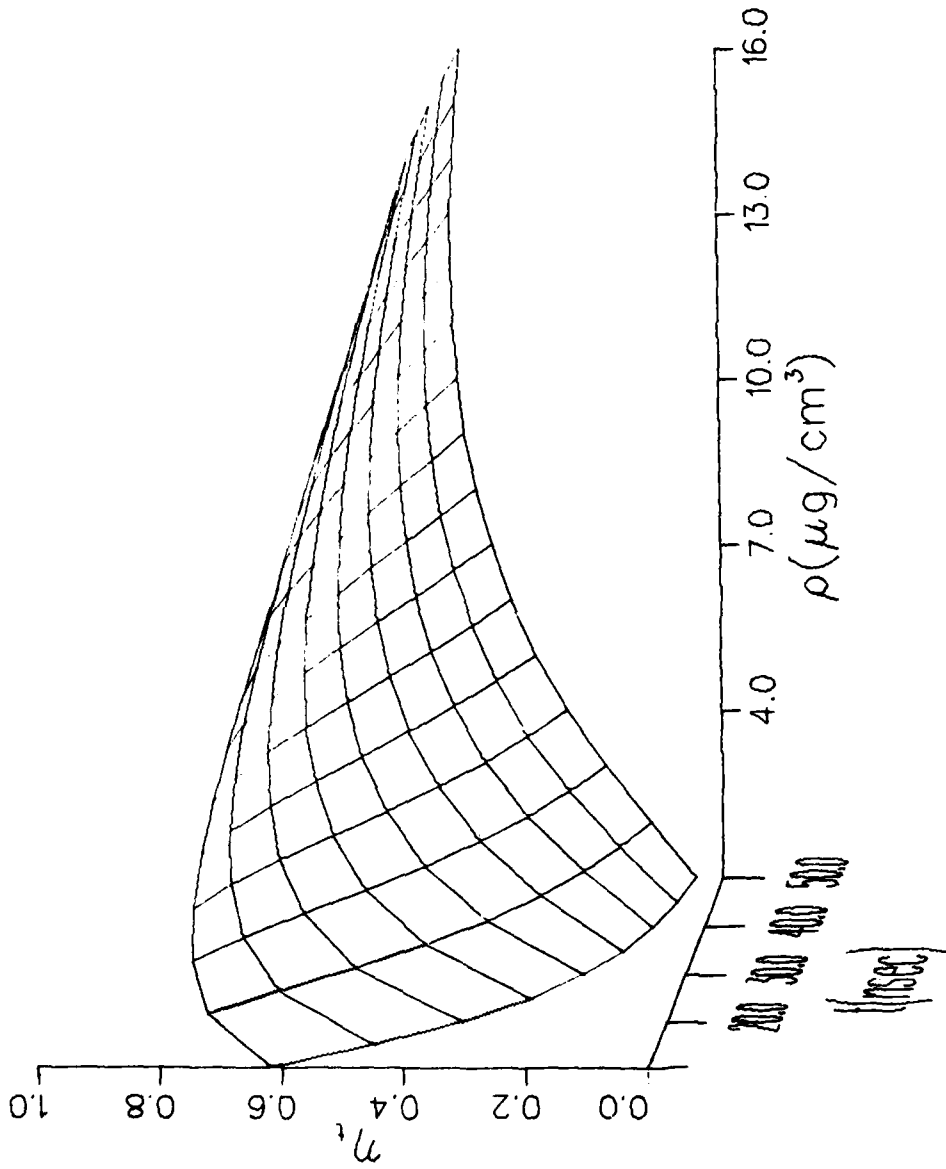


Fig. 5 — Total power density transport efficiency as a function of pulse duration and background channel density for the same parameters as in Fig. 1

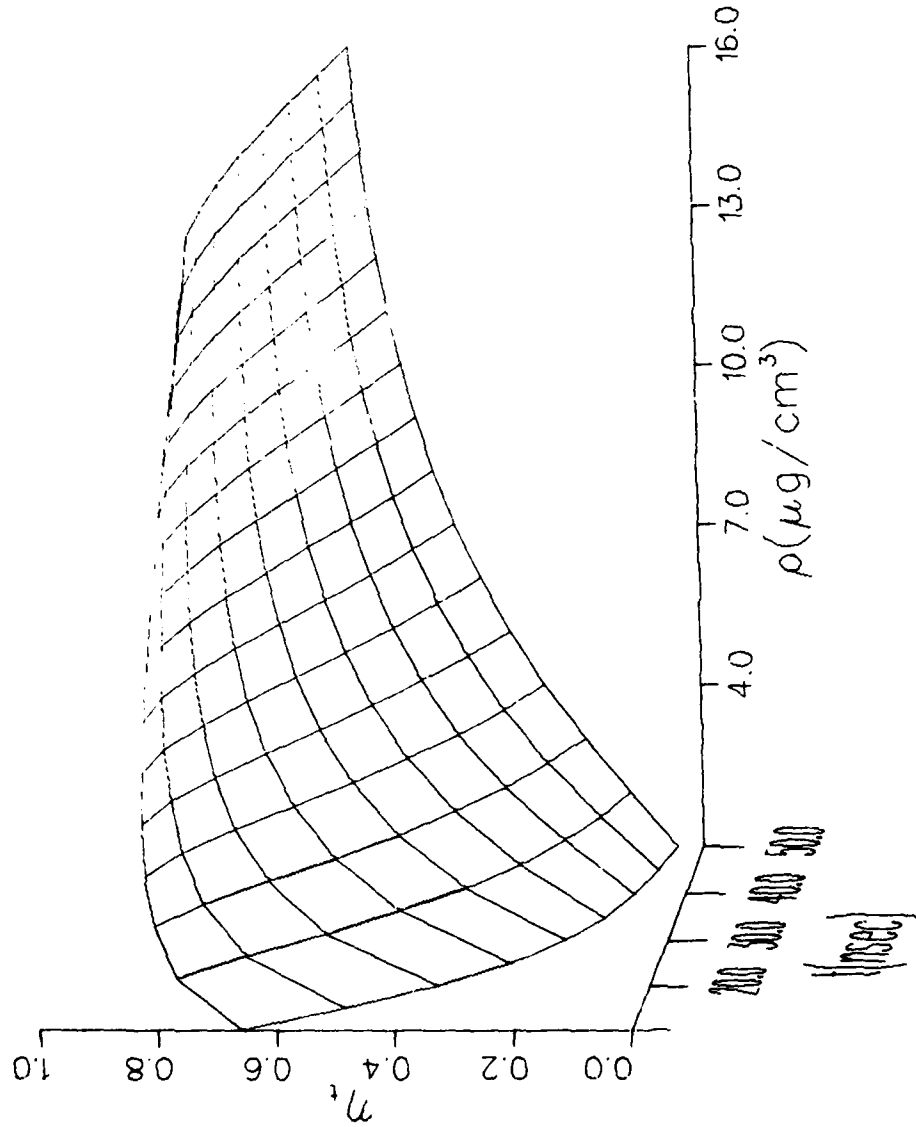


Fig. 6 — Same as in Fig. 5 for $\epsilon_b = 5$ MeV

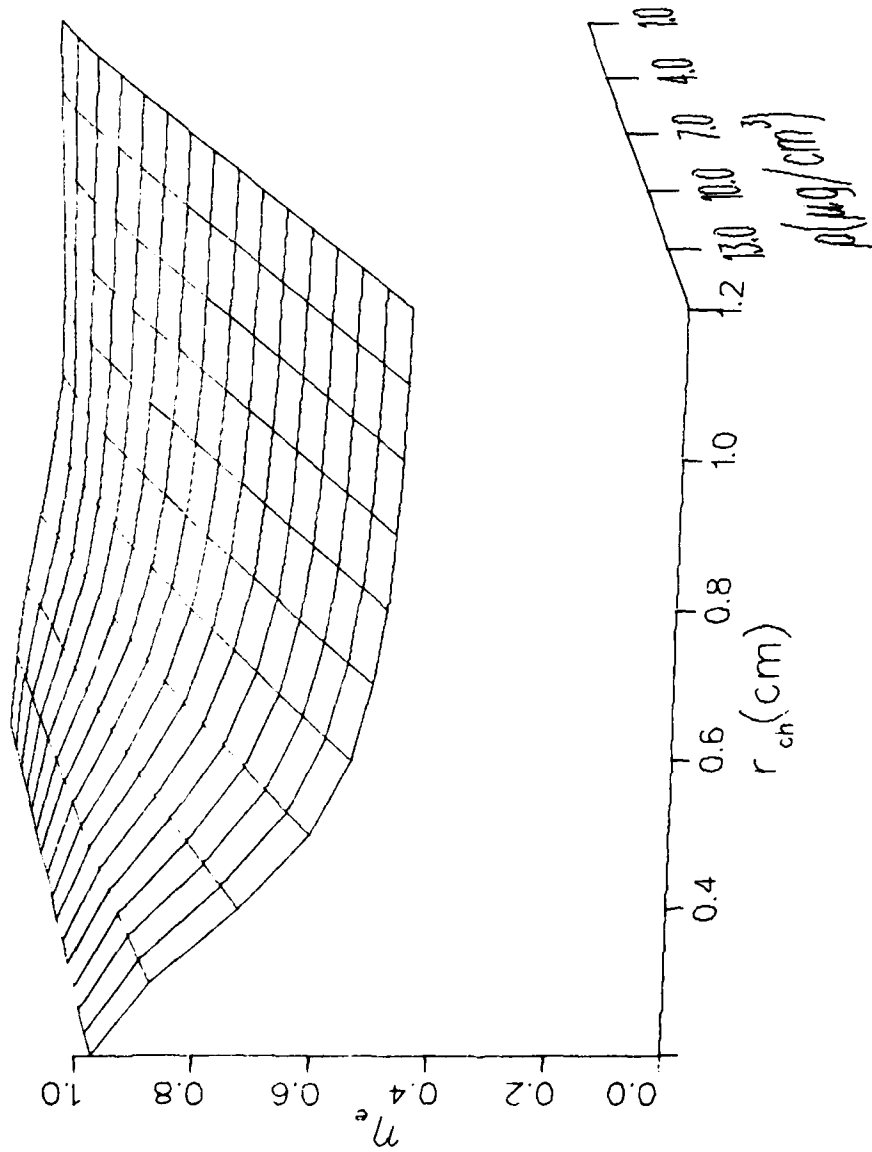


Fig. 7 — Energy transport efficiency as a function of background channel density and plasma channel initial radius for the same parameters as in Fig. 1 at $t = 40$ nsec

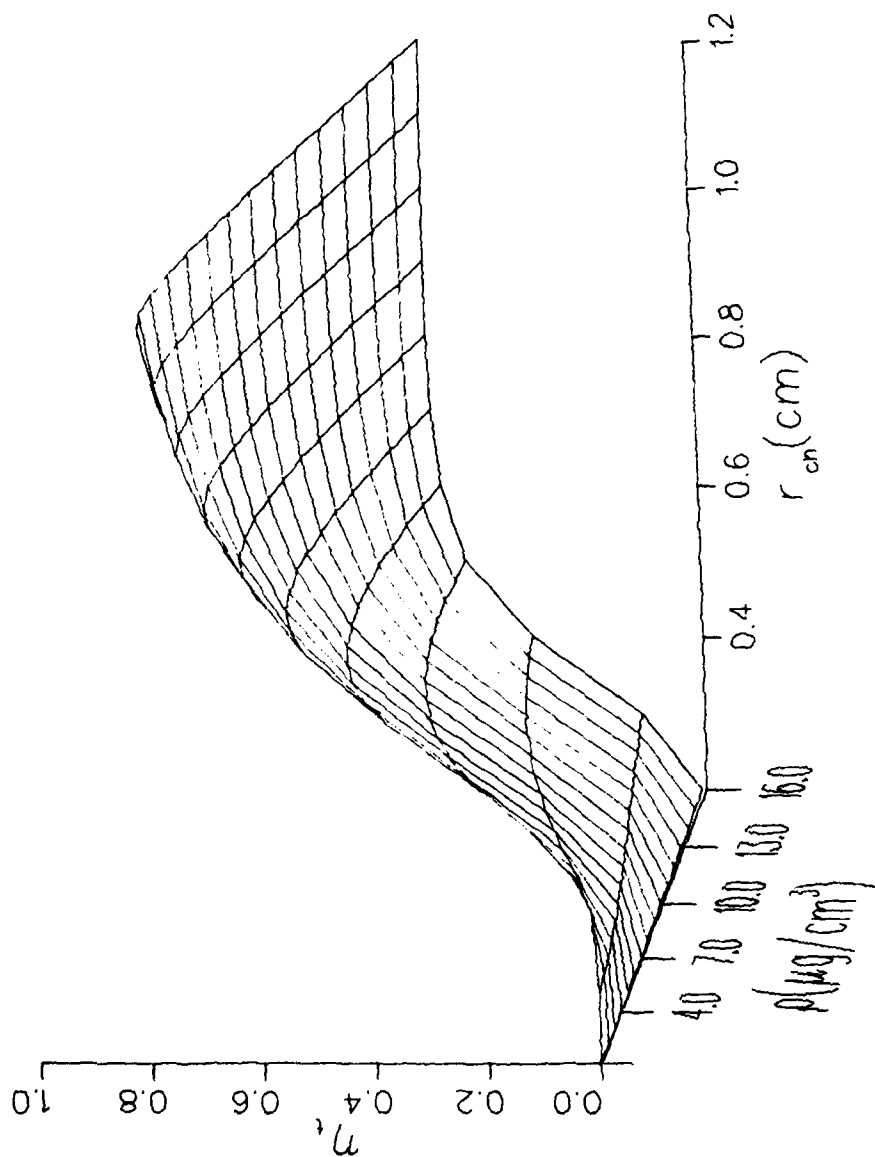


Fig. 8 -- Total power density transport efficiency for the case of Fig. 7

DISTRIBUTION LIST

Director
Defense Intelligence Agency
Washington, D.C. 20301
Attn: DTICI Robert I. Rubenstein

Defense Advanced Research Projects
Agency
1400 Wilson Blvd.
Arlington, VA 22209
Attn: R. Bayless

Director
Defense Nuclear Agency
Washington, D.C. 20305
Attn: FCPP
STVL
TISI Archives
TITL Tech. Library
(3 copies)
J. Z. Farber (PAFV)
P. L. Gullickson (PAFV)

Defense Technical Information Center
Cameron Station
5010 Duke Street
Alexandria, VA 22314
Attn: T. C. (12 copies)

Under Sec'y of Defense for RSCH
and ENCRS
Department of Defense
Washington, D.C. 20301
Attn: S&SS(OS)

Chief
Livermore Division FLD Command DNA
Lawrence Livermore National Lab.
P. O. Box 808
Livermore, CA 94550
Attn: FCPRL

National Technical Information
Service
U.S. Department of Commerce
5285 Port Royal Road
Springfield, VA 22161 (24 copies)

Commander
RMD System Command
P. O. Box 1500
Huntsville, AL 35807
Attn: SSC-TFM

Commander
Harry Diamond Laboratories
2800 Powder Mill Road
Adelphi, MD 20783
(CNWDI-INNER ENVELOPE)
ATTN: DFJHD-RRH)
Attn: DFJHD-VP
DFJHD-RCC J. A. Posado
DRYDC-RRH P. A. Caldwell
DRYDC-RRH D. Schallhorn
DRXDC-TI Tech Lib.
S. Graybill

Commander
Picatinny Arsenal
Dover, NJ 07801
Attn: SMIPA ND-N-F

Commander
U.S. Army Missile Command
Redstone Arsenal, AL 35899
Attn: Redstone Scientific
Information CTR
DPCPM-PM-PF-FA

Commander
U.S. Army Nuclear Agency
7500 Backlick Road
Building 2073
Springfield, VA 22150
Attn: ATCN-U

Commander
U.S. Army Test and Evaluation COMD
Aberdeen Proving Ground, MD 21005
Attn: DPSTF-FI.

Commander
Naval Electronic Systems CMD HOS
Washington, D.C. 20360
Attn: Code 5032

Commanding Officer
Naval Intelligence Support Center
4301 Suitland Road - Bldg. 5
Washington, D.C. 20390
Attn: NISC-45

DPP Chief of staff for RSCH DEV & ACC
Department of the Army
Washington, D.C. 20310
Attn: DAMA-CSM-M

Naval Research Laboratory
Attn: Name/Code
Washington, D.C. 20375
Addressee:
Code 2628 - TIC-Distribution (25 copies)
Code 4040 - J. Boris
Code 6682 - D. Nagel
Code 4700 - T. Coffey (26 copies)
Code 4707 - J. Davis
Code 4730 - S. Rodner
Code 4740 - V. Granatstein
Code 4760 - R. Robson
Code 4704 - C. Kapetanakis
Code 4770.1 - T. Vitkovitsky
Code 4771 - D. Mosher
Code 4773 - G. Cooperstein
Code 4790 - D. Colombant (10 copies)
Code 4790 - T. Haber
Code 4790 - P. Sprangle
Code 4790 - M. Lampe

Officer-in-Charge
Naval Surface Weapons Center
White Oak, Silver Spring, MD 20910
Attn: Code WR43
Code WA501-Navy Nuc Prgms Off

Chief of Naval Operations
Navy Department
Washington, D.C. 20350
Attn: P. A. Blaise 60404

Commander
Naval Weapons Center
China Lake, CA 93555
Attn: Code 533 Tech Lib.

AF Weapons Laboratory, AFSC
Kirtland AFB, NM 87117
Attn: CA
FLC
NT
SUJ
DVP
J. Darrah
W. L. Baker

HQ USAF/PD
Washington, D.C. 20330
Attn: PDOSM

Director
Joint Strat TCT Planning Staff JCS
OFFUTT AFB
Omaha, NB 68113
Attn: JSAS

SAMSO/DY
P. O. Box 92960
Worldway Postal Center
Los Angeles, CA 90009
(Technology) Attn: DYS

SAMSO/MN
Norton AFB, CA 92409
(Minuteman)
Attn: MNNH

SAMSO/SK
P. O. Box 92960
Worldway Postal Center
Los Angeles, CA 90009
(Space Comm Systems)
Attn: SKF P. H. Stadler

U.S. Department of Energy
Division of Inertial Fusion
Washington, D.C. 20545
Attn: C. Canavan (2 copies)
T. F. Codlove
S. L. Kahalas

Argonne National Laboratory
9700 South Cass Avenue
Argonne, Illinois 60439
Attn: G. R. Magelssen
P. J. Martin

Brookhaven National Laboratory
Upton, NY 11973
Attn: A. E. Maschke

Lawrence Berkley Laboratory
Berkeley, CA 94720
Attn: D. Keefe

Lawrence Livermore National Lab.
P. O. Box 808
Livermore, CA 94550
Attn: I-18
I-153
P. O. Rangerter
P. J. Briggs
F. P. Lee
J. H. Muckolls
S. S. Yu
Tech Info Dept. I-3

National Bureau of Standards
Washington, D.C. 20234
Attn: J. Leiss

National Science Foundation
Mail Stop 19
Washington, D.C. 20550
Attn: D. Berley

Sandia National Laboratories
P. O. Box 5800
Albuquerque, NM 87115
Attn: J. P. Freeman
S. Humphries
D. J. Johnson
C. W. Kuswa
P. S. Miller
J. P. Vandevender
C. Vonas
Doc Con for 3141 Sandia RPT Coll

AVCO Research and Systems Group
201 Lowell Street
Wilmington, MA 01887
Attn: Research Lib. A830 Rm. 7201

RDM Corporation, The
795 Jones Branch Drive
McLean, VA 22101
Attn: Tech Lib.

Boeing Company, The
P. O. Box 3707
Seattle, WA 98124
Attn: Aerospace Lib.

Cornell University
Ithaca, NY 14850
Attn: D. A. Hammer
P. N. Sudan
J. Maenchen

Dikewood Industries, Inc.
1000 Bradbury Drive, SE
Albuquerque, NM 87106
Attn: L. W. Davis

EC&C, Inc.
Albuquerque Division
P. O. Box 10218
Albuquerque, NM 87114
Attn: Technical Library

Ford Aerospace & Communications Corp
3939 Fabian Way
Palo Alto, CA 94303
Attn: Library
Dr. R. McMorrow MS C 30

General Electric Company
Space Division
Valley Forge Space Center
Coddard Blvd., King of Prussia
P. O. Box 8555
Philadelphia, PA 19101
Attn: J. C. Penden VFSC, Rm. 4230M

General Electric Company
Tempo-Center for Advanced Studies
816 State Street (P. O. Drawer 00)
Santa Barbara, CA 93102
Attn: DASTAC

Grumman Aerospace Corporation
Bethpage, NY 11714
Attn: P. Sub

Institute for Defense Analyses
400 Army-Navy Drive
Arlington, VA 22202
Attn: IDA Librarian P. S. Smith

Ion Physics Corporation
South Bedford Street
Burlington, MA 01803
Attn: H. Milde

Ian Smith Associates
3115 Gibbens Drive
Alameda, CA 94501
Attn: I. Smith (2 copies)

IRT Corporation
P. O. Box 81087
San Diego, CA 92132
Attn: P. L. Vertz

JAYCOR, Inc.
205 S. Whiting Street
Alexandria, VA 22304
Attn: J. Cuillory
P. Hubbard
P. Sullivan
D. A. Tidman
S. Goldstein (10 copies)

JAYCOR, Inc.
1401 Camino Del Mar
Del Mar, CA 92014
Attn: F. Venaas

Vaman Science Corporation
P. O. Box 7463
Colorado Springs, CO 80933
Attn: A. P. Bridges
D. H. Bryce
J. R. Hoffman
W. E. Ware

Lockheed Missiles and Space Co., Inc.
3251 Hanover Street
Palo Alto, CA 94304
Attn: L. F. Chase

MIT
Massachusetts Institute of Technology
Cambridge, MA 02139
Attn: P. C. Davidson
C. Bekefi
D. Hinshelwood

Maxwell Laboratories, Inc.
9244 Balboa Avenue
San Diego, CA 92123
Attn: R. W. Clark
A. C. Kolb
P. Korn
A. R. Miller
J. Pearlman

McDonnell Douglas Corporation
5301 Bolsa Avenue
Huntington Beach, CA 92647
Attn: S. Schneider

Mission Research Corporation
1400 San Mateo Blvd. SF
Albuquerque, NM 87108
Attn: R. B. Godfrey

Mission Research Corporation-San Diego
P. O. Box 1209
LaJolla, CA 92038
Attn: V.A.J. Van Lint

Mission Research Corporation
735 State Street
Santa Barbara, CA 93101
Attn: W. C. Hart
C. L. Longmire

Northrop Corporation
Electronic Division
2301 West 120th Street
Hawthorne, CA 90250
Attn: V. R. DeMartino

Northrop Corporation
Northrop Research and Technology Ctr.
3401 West Broadway
Hawthorne, CA 90205

Physics International Co.
2700 Merced Street
San Leandro, CA 94577
Attn: J. Benford
B. Bernstein
R. Cenuario
F. B. Goldman
A. J. Toepfer

Pulsar Associates, Inc.
11491 Sorrento Valley Blvd.
San Diego, CA 92121
Attn: C. W. Jones, Jr.

R&D Associates
P. O. Box 9695
Marina Del Rey, CA 90291
Attn: W. R. Graham, Jr.
M. Crover
C. MacDonald
F. Martinelli
L. Schlessinger

Science Applications, Inc.
P. O. Box 2351
LaJolla, CA 92038
Attn: J. Robert Revster

Spire Corporation
P. O. Box D
Bedford, MA 01730
Attn: R. C. Little

SRI International
333 Ravenswood Avenue
Menlo Park, CA 94025
Attn: Setsuo Odairiki

Stanford University
SLAC
P. O. Box 4340
Stanford, CA 94305
Attn: W. B. Herrmannsfeldt

Systems, Science and Software, Inc.
P. O. Box 4803
Hayward, CA 94540
Attn: D. A. Meskan

Systems, Science and Software, Inc.
P. O. Box 1620
LaJolla, CA 92038
Attn: A. R. Wilson

Texas Tech University
P. O. Box 5404 North College Station
Lubbock, TX 79417
Attn: T. L. Simpson

TRW Defense and Space Svs Group
One Space Park
Redondo Beach, CA 90278
Attn: Tech Info Center/S-1930

University of California
Dept. of Physics
LaJolla, CA 92037
Attn: K. Brueckner

University of California
Roelter Hall 7731
Los Angeles, CA 90024
Attn: F. F. Chen

University of California
Irvine, CA 92694
Attn: C. Benford
M. Postoker

University of Rochester
Laboratory of Laser Energetics
River Station, Hopeman 110
Rochester, NY 14627
Attn: Dr. Eastman

Vought Corporation
Michigan Division
39111 Van Dyke Road
Sterling Heights, MI 48077
Attn: Tech Lib

Bhabha Atomic Research Centre
Bombay - 400085, India
Attn: B. K. Godwal
A. S. Patilkar

CEA, Centre de Etudes de Valduc
P. R. 14
21120 Is-sur-Tille
FRANCE
Attn: J. Barbaro
C. Bruno
M. Camarcat
C. Patou
C. Peugnet

Ecole Polytechnique
Labo. PMT
91128 Palaiseau Cedex
FRANCE
Attn: J. M. Ruzzi
H. Doucet

Institut d'Electronique Fondamentale
Universite' Paris XI-Bat. 220
F91405 Orsay
FRANCE
Attn: G. Gautherin

Institut Fur Neutronenphysik
un Reaktortechnik
Postfach 3640
Fernforschungszentrum
D-7500 Karlsruhe 1
West Germany
Attn: H. H. Karow
W. Schmidt

Institute of Atomic Energy
Academia Sinica - Peking
People's Republic of China
Attn: R. Hong

Institute of Laser Engineering
Osaka University
Yamadakami
Suifu
Osaka 565, Japan
Attn: K. Imasaki
S. Nakai
C. Yamanaka

Instituto De Investigaciones Cientificas
Y Tecnicas De Las Fuerzas Armadas
Aufriategui y Varela
V. Martelli 1603
Pcia Bs. As. - R. Argentina
Attn: N. B. Carusso

Max-Planck-Institut fur Plasmaphysik
8046 Garching bei Munchen
West Germany
Attn: P. Jonvel

Physical Research Laboratory
Navrangpura
Ahmedabad - 380009 - India
Attn: V. Raman

Shivaji University
Kolhapur, India
Attn: L. N. Katkan

Weizmann Institute of Science
Rehovot, Israel
Attn: A. E. Blaugrund
F. Nardi
Z. Zinamon

SAMSO/IN
P. O. Box 92960
Worldway Postal Center
Los Angeles, CA 90009
Attn: IND MAJ D. S. Muskin

U.S. Department of Energy
P. O. Box 62
Oak Ridge, TN 37830 (50 copies)

University Illinois
Urbana, IL 61801
Attn: C. H. Miley
J. T. Verdevan

CFA, Centre d' Etudes de Limeil
B. P. 27
04100 Villeneuve Saint Georges
FRANCE
Attn: A. Bernard
A. Jolas

Los Alamos National Laboratory
P. O. Box 1663
Los Alamos, NM 87545
Attn: D. B. Henderson
P. B. Perkins
L. F. Thode

Ford Aerospace & Communications Operations
Ford & Jamboree Roads
Newport Beach, CA 92663
(Formerly Aeronutronic Ford Corporation)
Attn: Tech Info Section

**DATA
FILM**